Data Analysis Results from the GOLD Experiments

M. Jeganathan, M. Toyoshima[a], K. Wilson, J. James[b], G. Xu [c] and Lesh

Jet Propulsion Laboratory
4800 Oak Grove Dr
Pasadena, CA 91109

[a]Communications Research Laboratory
Koganei, Tokyo, Japan

[b]New Mexico State University
Las Cruces, NM 88003

[c]California Institute of Technology
Pasadena, CA 91125

ABSTRACT

Analyses of uplink and downlink data from recent free-space optical communications experiments carried out between Table Mountain Facility (near Pasadena, CA) and the Japanese ETS-VI satellite are presented. Fluctuations in signal power collected by the satellite's laser communication experiment (LCE) due to atmospheric scintillation and its amelioration using multiple uplink beams are analyzed and compared to experimental data. Downlink data was analyzed to determine the cause of a larger than expected variation in signal strength. In spite of the difficulty in deconvolving atmospheric effects from pointing errors and spacecraft vibration, experimental data clearly indicate significant improvement in signal reception on the uplink with multiple beams, and the need for stable pointing to establish high data rate optical communications.

Keywords: Free-space optical Communication, Atmospheric Scintillation, Multi-beam Uplink, Downlink, Aperture Averaging, Laser Communication, Link Budget

1. INTRODUCTION

An optical communication link between an Earth-orbiting satellite and a ground based receiver involves propagation of laser beam through the atmosphere. Spatial and temporal variations in the index of refraction of the air that forms the atmosphere severely degrade the quality of the beam. These variations, typically lasting in the order of one thousandth of a second at optical and near IR frequencies, in index of refraction result in random changes in the amplitude and phase of the arriving wave. The amplitude and phase fluctuations manifest themselves in effects such as scintillation), beam broadening and beam motion or wander. Scintillation can be thought of as interference between partial waves propagating through different paths (or turbulent cells), which result in fades (destructive interference) or surges (constructive interference) at the receiver. Beam motion, primarily on the uplink, can often be considered as atmospheric-induced jitter in pointing of the laser beam. Such motion of narrow beams can cause deep fades in the signal due to the Gaussian nature of the spatial beam profile. Deep fades causing signal loss or strong surges causing saturation of the quad-detector can force loss of track On the uplink, with the exception of heavy cloud cover, atmospheric scintillation is usually the limiting factor in an optical link. For downlink, however, the large size of the receive aperture typically compensates for scintillation by averaging over fades and surges.

In addition to atmospheric-induced signal variations there are other variations in signal caused by spacecraft vibration, tracking error and pointing jitter. These errors depend largely on the characteristics of the optical communications system both on the satellite and ground, Without a detailed understanding and characterization of the

Send all correspondence to Muthu Jeganathan
Email: muthu@altair.jpl.nasa.gov; Telephone: **818-354-9100**; Fax: **818-393-6142**
Supported by NASA under Contract

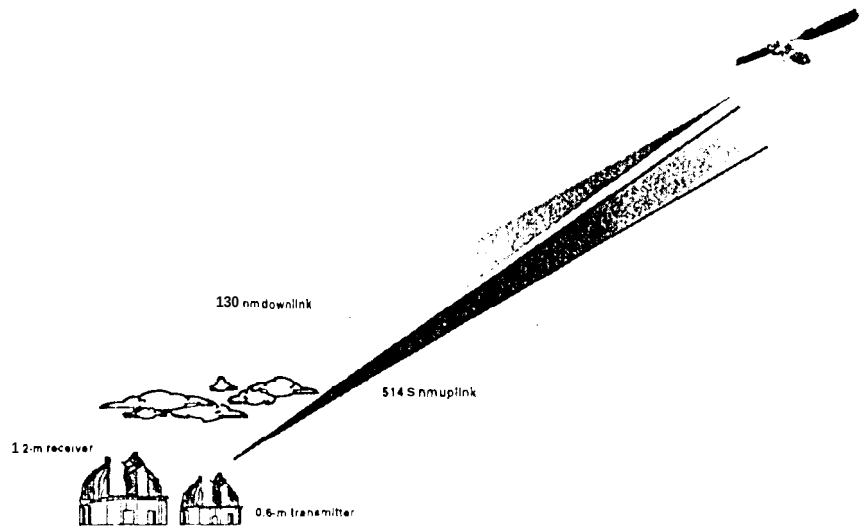

Figure 1. Figure showing laser communication link between TMF and the ETS-VI satellite

optical system, it is impossible to identify the statistical properties of atmospheric effects. Assuming that these atmospheric effects are well described by existing models, the difference between experimental and predicted performance is then primarily due to the optical communication system itself.

In this paper we use data from the recent Ground/Orbiter Lasercomm Demonstration (GOLD) experiments to study the atmosphere-induced fluctuations in signal power both on uplink and downlink. The experiment's objective was to establish an optical communication link at 1.024 Mbps between the Laser Communication Experiment (LCE) onboard the Japanese ETS-VI satellite and the Table Mountain Facility (TMF) near the Jet Propulsion Laboratory (JPL). The link was established by first transmitting a beacon from TMF to ETS-VI using a priori knowledge of the satellite's orbit. The beacon was subsequently acquired and tracked by the LCE package on the satellite. Once the tracking loop was activated on the LCE, the onboard *laser* was turned on and its beam was pointed to the ground station for downlink. The downlink beam was then detected by the receiver at TMF to complete the link. Once the link was established, both the downlink laser and uplink beacon could be modulated for transmission of data. A good description of the GOLD experiments, details on the LCE can, and results of other optical communications experiments carried out with the LCE can be found in References [1-4]. Our focus in this paper is more on the signal fluctuations, both on uplink and downlink, and less on the communication aspects of the link.

The reminder of the paper is divided primarily into two parts: Section 2 deals with uplink while Section 3 deals with the downlink. For the uplink, we begin in section 2.1 with a brief summary of the theory that describes beam propagation through free-space, atmospheric scintillation and effects of multiple uplink beams. Section 2.2 provides the specifics of the experiments and a typical link budget for the uplink. The experimental uplink data is presented and compared to theory in Section 2.3. For the downlink, we discuss the probability distribution due to pointing jitter in section 3.1. A typical link budget for downlink is presented in Section 3.2 and the corresponding experimental results are presented in Section 3.3.

2. UPLINK

2.1. Theory

Consider a communication channel between a ground station and an orbiting satellite that is specific to GOLD as shown in Figure 1. A detailed discussion of the influence of the atmosphere on the statistics of the channel during beacon uplink follows.

We can consider the power, P_R, received by the photodetector on the satellite to be the product of three quantities:

$$P_R = P_0 I S$$

where P_0 is the power received in the absence of a turbulent atmosphere, I is a random variable with a beta-distribution caused by atmospheric and pointing jitter, and S is typically a log-normal random variable due to scintillation. The maximum receivable power, P_0 at the satellite was assumed to have zero variance. Thus fluctuations due to the laser and detector noise are assumed to he negligible compared to scintillation and beam jitter. In the following sections, the major contributions to the observed statistics of the received power on the uplink are described.

2.1.1. **Free-space** propagation

For an optical transmitter with continuous wave (CW) laser power of P_T Watts, the power received by the detector onboard the satellite in the absence of atmospheric turbulence is primarily governed by free-space-propagation loss and optical absorption and is given by:

$$P_0 = \eta G_T \cdot G_R L_s P_T \tag{1}$$

where η is a combined loss term which accounts for transmitter and receiver optical loss, atmospheric loss and pointing loss; G_T is the transmitter gain which depends on transmit beamwidth; G_R is the receiver gain which depends on receiver or collector area and wavelength; L_s is the space loss which depends on the wavelength and the distance between the transmitter and receiver. The expressions for gains and losses are well known and shall not be presented here (see the link table in the following section for the values of gains and losses). It must be noted that the concept of gain is more often used in RF communications analysis than in optical communications. At optical frequencies, it is common to drop the wavelength dependence of receiver gain and space loss and instead replace them with collector area and propagation loss, respectively. That is, the received power is written as:

$$P_0 = \eta \left(\frac{2.44\pi}{\theta} \right)^2 \left(\frac{D_R}{4r} \right)^2 P_T \tag{2}$$

where θ is the beamwidth in radians; D_R is the receiver aperture diameter in m and r is the transmitter-to-receiver range in m. In this expression, the effects of obscuration and truncation have been ignored and the beam width refers to full-width to first null of the Airy beam pattern.

We may to a good approximation assume that all quantities in the above equation are constant over the duration of the experiment which typically last few hours. That is, we assume that the communication range, observation angle, atmospheric transmission, etc. change little in the 2-4 hours of an experimental pass. In the presence of thin moving clouds, however, atmospheric transmission can vary significantly over such a long duration.

2.1.2. Light Wave Propagation in Turbulent and Random Media

Wave propagation through lossless random media, like the atmosphere, is often characterized by the structure constant C_n^2 , which is a measure of the variance of the index of refraction due to inhomogeneities in the medium [5]. For modeling the atmosphere, one often needs to know the altitude variation of the structure constant and its dependence on weather conditions. Though modeling the atmosphere is a difficult task, there exist several empirical and parametric models for the altitude variation in the structure constant of the atmosphere. The most common of these is the theoretically based Hufnagel model in which the dominant turbulence arises from winds in the 5-20 km altitude range [6]. The altitude of TMF (2.2 km above sea level) is well outside the range of validity of the Hufnagel model (over 3 km above sea level). The validity of the improved Hufnagel-Valley 5/7 model, which includes a boundary layer term, on the other hand, extends down to the ground [7]. This model, however, predicted a larger than observed turbulence at TMF by overestimating the low altitude contribution. We, thus, used the experimentally based AFGL CLEAR I night model [8]. The CLEAR I night model was based on the average of a large number of measurements of the atmospheric properties in the New Mexico Desert. The model provides the functional dependence of C_n^2 on altitude down to 1.23 km above mean sea level:

$$\log(C_n^2) = A + Bh + Ch^2 + D\exp\left(-\frac{(h-E)^2}{2F^2} \right) \tag{3}$$

where h is the altitude in km above mean sea level. The constants A, B, C, D, E and F are defined for three different ranges of altitude and listed in Chapter 2 of Ref. [8]. host quantities of interest such as the scintillation variance are usually expressed as weighted integrals of the index of refraction structure constant, as described below.

Consider, for example, observation of a star with a large aperture telescope. As noted earlier, the large aperture negates the effect of scintillation by averaging over constructive and destructive interferences. Since light from a distant object can well be approximated by plane waves, the only prominent effect of the turbulent atmosphere is thus the change in the angle of arrival of the plane wave. The random arrival angle limits the resolution of the telescope. In fact, the resolution of the telescope is equivalent to the resolution of an aperture, r_0 (called the coherence length of the atmosphere), determined by the atmospheric structure constant and wavelength of light [9]:

$$r_0 = \left[0.423k^2 \sec\theta \int_{h_0}^{\infty} C_n^2(h)dh\right]^{-3/5} \tag{1}$$

where $k = 2\pi/\lambda$ is the wavevector of the plane wave, h is the height above sea level and h_0 is the altitude of the location of the telescope. From basic principles of optics, an aperture with diameter r_0 has a full-width-half-maximum (FWHM) angular resolution of :

$$\text{Angular resolution} = \frac{\lambda}{r_0}$$

For a wavelength of 0.5 microns, the coherence length r_0 is on the order of 10 cm. In experimental observations, it is convenient to define "seeing" as the full-width-half-maximum (FWHM) of the angular spread of the star. For r_0 of 10 cm, the seeing is approximately one arc-second or 5 micro-radians. It must be noted that though sub-arc-second seeing conditions are possible at TMF, a more representative value for the seeing at TMF is 2-3 arc seconds, or an r_0 of little under 5 cm.

Given the AFGL model for the altitude dependence of the structure constant, the above equation for r_0 gives a single value for the atmospheric coherence length irrespective of the meteorological conditions. To better model the existing local weather conditions, we scale the structure constant function by a multiplicative constant so that the predicted value of r_0 matches the r_0 derived from measured seeing. The scaled C_n^2 was then used to determine other atmospheric related quantities such as scintillation variation and beam wander. For this purpose, the seeing was measured several times during a single run of the GOLD experiment.

2.1.3. Atmospheric Scintillation

The PDF of the normalized received intensity, S, at a point receiver due to scintillation can take several forms. For weak turbulence, S is proportional to $\exp(2\chi)$ where χ is the log-amplitude of the wave. Since χ is a normally distributed random variable, the transformation $S = \exp(2\chi)$ results in S being a log-normal RV. The quantity 2ξ is often referred to as the log-irradiance and the variance of χ is referred to as the log-variance of S. For strong turbulence over long paths, the intensity fluctuations are severe and the distribution is exponential. Andrews and Phillips have shown that scintillation can be described by an I-K distribution (i.e., containing I and K Bessel functions) which reduces to the two limits given above for weak and strong turbulence [10,11]. Since the GOLD experiments were performed at relatively high altitudes (2.2 km for TMF) and the source of most turbulence is at or near sea level, we assume a weak turbulence model and use the log-normal distribution for S. That is,

$$f_S(s) = \frac{1}{\sqrt{2\pi\sigma_l^2}} \frac{1}{s} \exp\left[-\frac{1}{2\sigma_l^2}(\ln s - l_m)^2\right] \tag{5}$$

where $l_m = -\sigma_l^2/2$ is the mean of the log-irradiance distribution. The quantity S, being a normalized quantity, has a mean of 1. The variance of the log-irradiance is determined from the following weighted integral of the index of refraction structure constant [12,13]:

$$\sigma_l^2 = 2.24k^{7/6}(\sec\theta)^{11/6} \int_{h_0}^{\infty} C_n^2(h)h^{5/6}dh \tag{6}$$

where k, h and h_0 are as defined before. Experiments have shown that σ_l^2 does not arbitrarily increase with increasing atmospheric turbulence. In fact, the scintillation variance reaches a saturation value of approximately $\sigma_\chi^2 = \sigma_l^2/4 = 0.3$ [14]. The variance of S itself is given by

$$\sigma_S^2 = \exp\sigma_l^2 - 1 \tag{7}$$

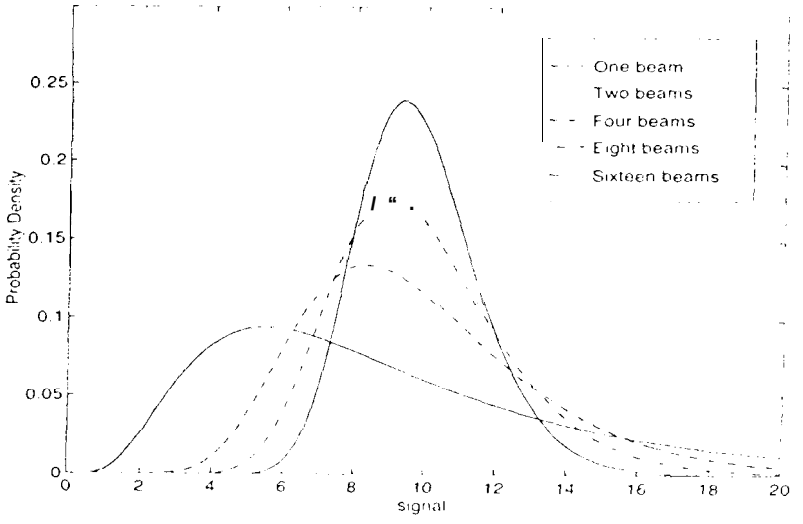

Figure 2. PDF of the received signal intensity, S, showing the improvement in variance with multiple uplink beams.

Note that it is customary to characterize the log-normal distribution of S using the mean and variance of the log-irradiance. Thus neither the mean nor the variance of S is immediately apparent from $f_S(s)$.

For the case of uplink, we shall assume that the pointing jitter was negligible compared to scintillation effects. That is, both the atmosphere-induced beam wander and pointing jitter were assumed to be low. Thus the received power can be written as:

$$P_R = \eta \left(\frac{2.44\pi}{\theta_t} \right)^2 \left(\frac{D_R}{4r} \right)^2 P_t S \tag{8}$$

We emphasize that in the above equation P_R and S are RVs. For the case at hand, we proceeded with the assumption that scintillation was the primary cause for signal variation.

2.2. Effect of Multiple-uplink-beams

The adverse effect of scintillation can be reduced by the use of multiple uplink beams, each incoherent with the rest and separated by a distance larger than the atmospheric coherence diameter r_0. That is, each beam produces its own independent speckle pattern and the detector sums over fades and surges from the different beams. For such a case, the signal arriving at the detector is the sum of the signal from each uplink beam with independent-identically-distributed (IID) statistics. That is

$$S = \sum_{n=1}^{N} \hat{S}_n \tag{9}$$

where N is the number of independent beams, and the random variables S_n are log-normally distributed. We assume that the total uplink power remains constant and thus each beam, $\hat{S}_n$, has 1/Nth of the total power. From the properties of sums of IID random variables, we find that S is a convolution of N log-normal distributions. Analytic expressions for the convolution of log-normal functions are unavailable, and thus we resort to numerical techniques using characteristic functions and Fast-Fourier-Transforms (FFT). Note that for large N, according to the central limit theorem (CLT), the distribution of S approaches a Gaussian.

To illustrate the benefits of launching multiple beams during uplink, we choose, as an example, a mean of $10/N$ and log-variance of 0.4 for each S_n. Figure 2 shows the expected PDF when total laser power is equally distributed in one, two, four, eight or sixteen beams. Several features are worth noting. First, the means for all the distributions are the same. Second, the location of the peak of the PDF approaches the mean of S when N is increased. Finally,

Link **Range**	**38000**	k m			
Data rate	1024.0	kbps	Binary PPM or Manchester		
			Transmitter (TMF)		
Laser (Argon-ion)					
Peak power			**13.20 W**	41.21	dBm
Average power	660	w			
Wavelength	**51450**	nm			
Energy perpulse	644531	nJ			
Telescope (1'kIt-' 24-inch)					
Gain			**2 42E+I0**	**10383**	dB
1ransmitbeamwidth	*30.00*	µrad			
Telescope optical **losses**			**0.75**	**-1.25**	dB
			Channel		
Space loss			1.16E-30	**-299.35**	dB
Atmosphere					
Transmission			**0,49**	**-3.1'1**	dB
Transmission at zenith	60.00	%			
Observation angle from zer	45.00	degrees			
			Receiver (GEO)		
Telescope (LCE on ETS-VI)					
Gain			21 0E+11	113,22	dB
Aperture diameter	7.50	cm			
Other losses			**0.15**	**-8.24**	dB
			Link Summary		
Power received at detector			**4.24 nW**	**-53.73**	**dBm**
Required power at detector			**0.63 nW**	**-62.01**	**dBm**
Link margin			**6.73**	**8.28**	**dB**

Table 1. Link budget for TMF to LCE transmission.

the PDF is concentrated around the mean for large values of N. In short, though the mean does not vary with increasing number of beams, the variance drops significantly with additional beams. In fact, for the example in Figure 2, the probability of greater-than-3-dB-fades from the mean drops from over 22% for one beam to just over 3% for four beams.

In the presence of strong scintillation, dividing the laser power into several beams is essential to avoid deep fades and surges. The number of beams needed to achieve a given bit error rate (BER) will depend on the strength of the scintillation. Part of the objective of GOLD was to understand the effects of multi-beam propagation through the atmosphere. In the GOLD experiments, light from the laser was split into two or four and the path length difference between the beams was increased to a distance greater than the coherence length of the laser. The beams were then launched into the coude so as to emerge from the primary separated by a distance of 20 cm (which was much greater than r_0). Thus the actual variance of the received signal would have been less than that predicted by the single-beam model.

2.3. Link Budget

One of the objectives of the GOLD data analysis was to compare the observed mean and variance of the uplink signal to the predicted values. The link budget of Table 1 shows the expected mean value of received signal for transmission of a single high power CW beam from TMF up to the satellite. The link budget is for the avalanche photo-diode (APD) in the communication channel of the LCE.

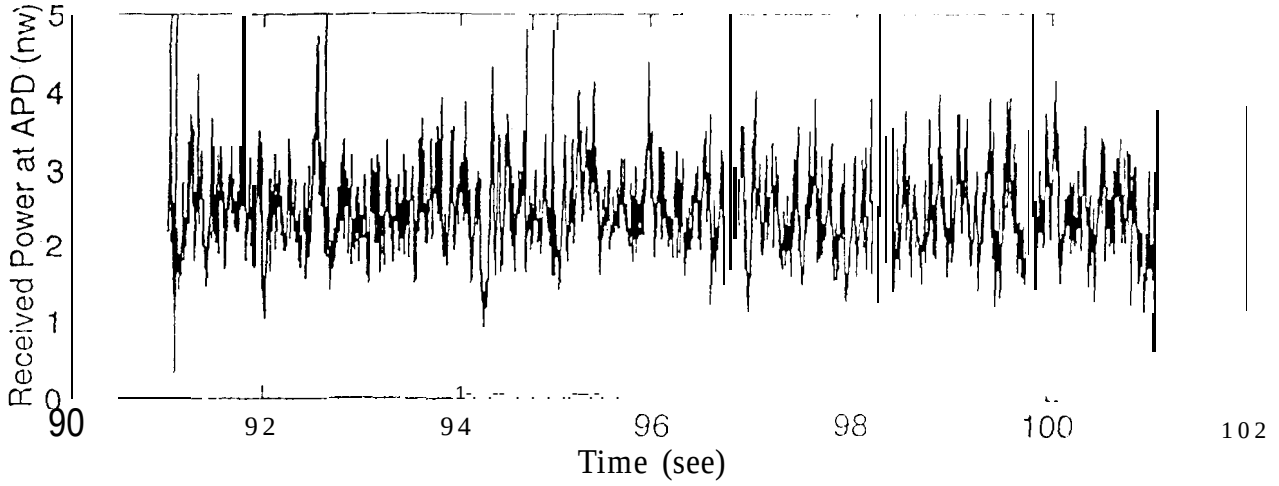

Figure 3. Uplink signal fluctuations observed over a 10-sec time interval on May 12, 1996. The large spikes are due to errors in the "E2" frame

All data concerning the laser communication package on the satellite was provided by the Communication Research Laboratory (CRL) in Japan. Parameters pertaining to TMF transmitter were determined experimentally or estimated from telescope properties. Values of parameters such as range and elevation were typical values for the duration of the experiments. Finally, background radiation from earth reaching the detector was negligible as most experiments were conducted at night from TMF. Losses due to pointing bias and jitter were not included in the link table but are expected to be about 2 dB.

2.4. Experimental Data and Analysis

The LCE onboard the ETS-VI satellite had three photo detectors: a CCD for acquisition; a quad-photo-detector for tracking and an APD for communication. There were two sets of data available to us from these three detectors - one from the S-band telemetry and the other from the optical downlink carrier. Data from the S-band telemetry contain CCD and QPD signals sampled every second. Thus even though the CCD frame rate was 30 Hz and the QPD bandwidth was tens of Hz, the available data was only at 1-Hz interval. In addition, the QPD data (which was the sum of the signal from the four quadrants) showed significant saturation except on few days. A preliminary analysis of CCD and QPD data can be found in Ref. [15].

Due to the aforementioned reasons it was better to use the APD data sent via the optical carrier, which was sampled at 500 Hz. It must be noted that the APD current sensor circuit had a bandwidth of only about 40 Hz. Data from an additional 400 Hz bandwidth APD circuit also showed significant saturation to be of much use. The LCE downlink status had to be in the "E2" (or telemetry) mode instead of the PN (pseudo-random noise) or regeneration mode to obtain the APD data. Furthermore, there were very few instances of stable downlink over extended periods of time due to spacecraft pointing. In this article we use available APD data (from the 40 Hz bandwidth circuit) extracted from the "E2" telemetry to analyze uplink signal fluctuations [16].

Figure 3 shows a plot of the power detected by the APD over a 10-sec time interval when the uplink beam was divided into four beams, each mutually incoherent and separated by 20 cm. The mean of the received power was about 2.4 nW. This compares well to the 2.1 nW of average power (4.2 nW peak power) predicted in the link table. The discrepancy between the predicted and observed mean values was just about 0.6 dB. The agreement between theory and experiment for the mean value was surprisingly good given the various unknown factors such as the exact value of the atmospheric transmission, transmitter pointing offset and jitter. The normalized variance of the signal, on the other hand, was 0.045 and will be discussed shortly.

Figure 4 shows the PDF of the signal in Figure 3 for a four-beam uplink. Since no expressions are available for convolutions of log-normal distribution, we could not easily fit the experimental data. We, therefore, used a log normal distribution with mean and variance one-quarter of what was observed experimentally with four beams. When this log-normal distribution was convolved with itself four times we obtained the smooth curve shown in Figure 4. The mean and Valiance, of course, are the same for the two curves. The important thing to note is the strikingly similar functional form of the two curves. This indicates that the log-normal distribution for scintillation predicted by the weak-turbulence model of tile atmosphere was indeed a good one. From the experimental data we

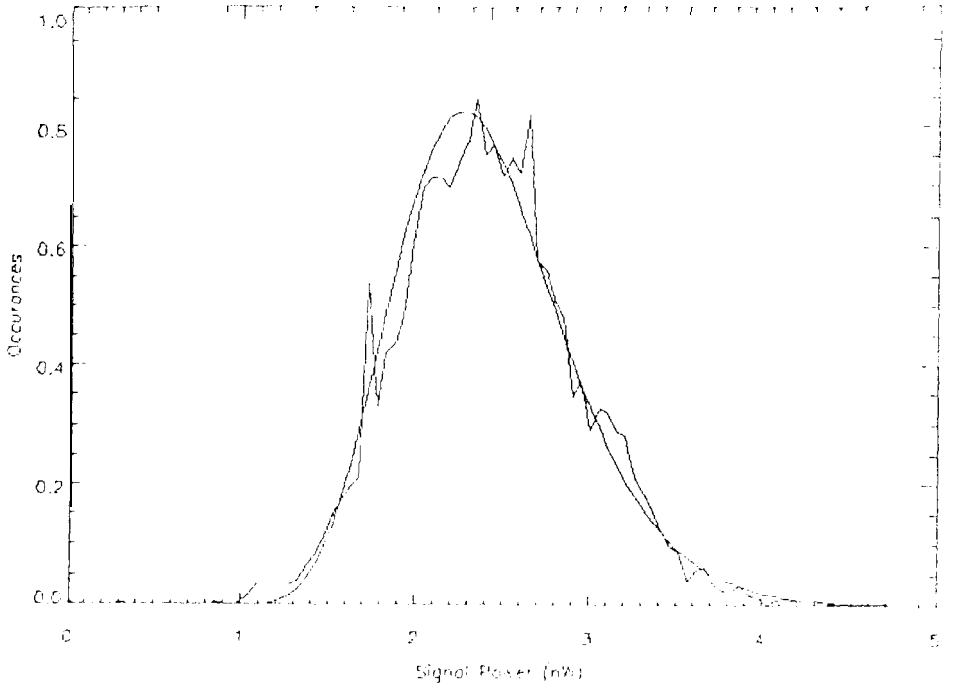

Figure 4. Probability distribution function of uplink signal shown in previous figure. The smooth curve overlayed on the PDF is the convolution of four log-normal distributions (see text).

see that if only one beam were sent up instead of four, the normalized variance would have been 0.18. From Eq. 8, the log-variance would have been $\sigma_I^2 = 0.17$. That corresponds to a seeing of about 3 μrad which was smaller than the approximate 1.5 arc-sec seeing measured at TMF on May 12, 1996. The difference could be due to the different times at which the seeing and uplink measurements were made.

3. DOWNLINK

3.1. Theory

The receiver aperture diameter used for GOLD downlink was 1.2 *m*. Hence the receiver encompasses a large number of atmospheric coherence cells which are typically in the order of several cm as described earlier. This averaging over many constructive as well as destructive interference cells nearly eliminates the effects of scintillation on the downlink and is called aperture averaging. The dominant causes of signal fluctuations are then pointing jitter and atmosphere-induced beam motion.

3.1.1. Beam Motion and Jitter

To account for intensity fluctuations due to pointing inaccuracies and beam wander, we assume a Gaussian intensity profile for the uplink laser beam. That is, the normalized intensity pattern takes the form:

$$I(\delta_x, \delta_y) = \exp\left[-4\left(\frac{\delta_x^2 + \delta_y^2}{\theta^2}\right)\right] \tag{10}$$

where δx and δy are the angular deviation or error in the pointing. If the transmitter and receiver are *on-axis* and there is no pointing offset ($\delta x = \delta y = 0$) the receiver would see a power P_0 from the transmitter. Because of pointing jitter and atmospheric induced beam motion, however, δx and δy are random variables and not constants. We assume dx and dy to be identically and normally distributed with zero mean and variance σ_J^2. The variance σ_J^2 of the jitter is the sum of the variance of atmospheric-induced and transmitter-induced pointing errors.

The new random variable I can be shown to have the following cumulative probability distribution function (CDF) [17]:

$$P_I(I \leq i) = F_I(i) = i^\beta \text{ for } 0 < i < 1 \tag{11}$$

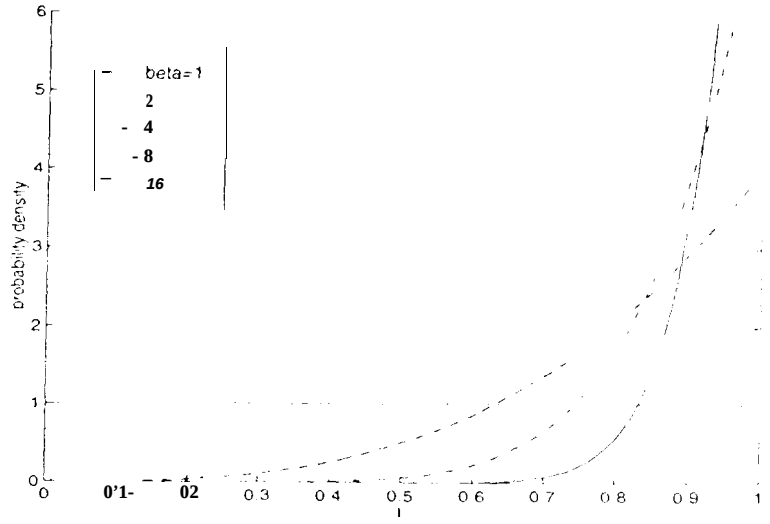

Figure 5. PDF of signal due to pointing jitter. Figure shows the β-distribution for several different values of β

where

$$\beta = \frac{1}{8}\left(\frac{\theta}{\sigma_J}\right)^2 \tag{12}$$

is a measure of the pointing accuracy with respect to the beam width. We immediately see that the mean and variance of I are given by $< I >= \beta/(\beta+1)$ and

$$< I^2 > - < I >^2 = \frac{\beta}{(\beta+1)^2(\beta+2)}$$

respectively. It is obvious that a large value of β is desirable. In fact, for large values of β, the mean approaches the optimum value of one and the variance tends to zero as $1/\beta^2$. For small values of β ($\beta \ll 1$), on the other hand, both the mean and variance are proportional to beta. Figure 5 shows the PDF due to pointing jitter for different values of beta. Note the sharp fall off (discontinuity) at $I = 1$ due to the fact that the received power can never be greater than when pointed properly.

To achieve a large value of β, either the angular beamwidth must be increased or the beam jitter must be decreased. With less control over the beam jitter, one is often limited in practice to increasing the beam divergence for obtaining a particular value of beta. But the received power is inversely proportional to the square of the beam divergence. An optimum value of β, therefore, exists and depends on the magnitude of the jitter. The statistical analysis of the effect of a constant pointing offset is complicated by the loss of circular symmetry. For simplicity, we accounted for constant pointing offset only through an exponential loss factor.

3.2. Link budget

Table 2 shows a link budget for the downlink similar to the one for uplink. In fact, most of the parameters are about the same for uplink as well as downlink. The substantially lower power of the LCE's transmitter was compensated for in the link by the substantially larger collector area, resulting in an approximately same value of received power for both uplink and downlink.

3.3. Experimental results

Before getting into the experimental results, it is necessary to describe some of the experimental details of the transmitter and ground receiver. First, a 20% 8-kHz modulation was impressed upon the downlink signal. This provided a carrier frequency for the downlink and proved very useful in analyzing the downlink signal. Second, an

Link Range	**38000**	**km**			
Data rate	**1024.0**	kbps	**PPM (M = 2)**		
			Transmitter (GEO)		
Laser (LD:830)					
Peak power			**0.028 W**	14.41	dBm
Average power	0.014	W			
Energy per pulse	**1348**	nJ			
Relay Optics					
Losses			**0.30**	**-5.23**	dB
Telescope (LCE on ETS-VI)					
Gain			**242E+1O**	**10383**	dB
Transmit beamwidth	**30.00**	µrad			
			Channel		
Space loss			3 **24E-30**	**-29489**	dB
Atmosphere					
Transmission			O **60**	**-219**	dB
Transmission al zenith	**7000**	%			
Observation **angle from** zer	**45.00**	**degrees**			
			Receiver (TMF)		
Telescope (TMF 48-inch)					
Gain			1.84E+13	13264	dB
Aperture diameter	**120.00**	cm			
Filter loss			**O 80**	-097	dB
Other losses			**0,64**	-1.94	dB
			Link Summary		
Power received at detector			**3.69 nW**	**-54.33**	**dBm**
Required power at detector			**0.70 nW**	**-61.55**	**dBm**
Link margin			**5.27**	**7.22**	**dB**

Table 2. Link budget for TMF to LCE transmission.

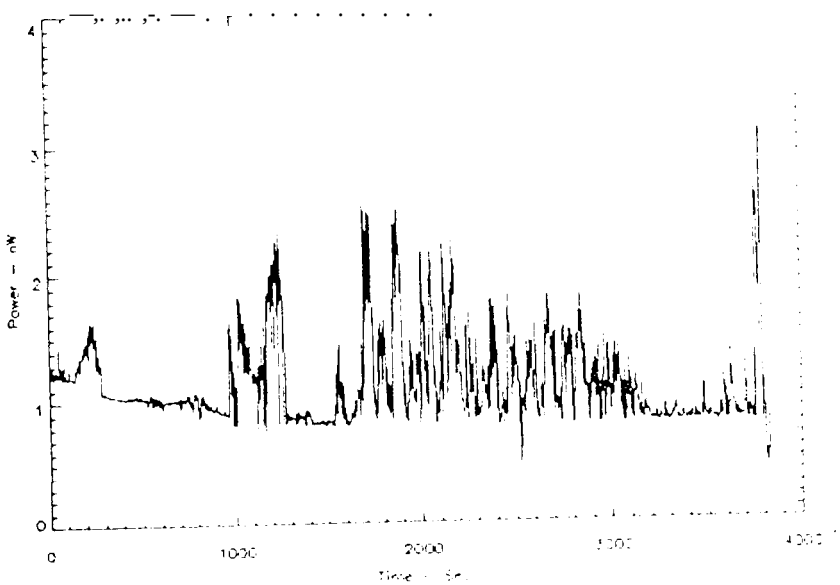

Figure 6. Downlink signal fluctuations with time observed on May 12, 1996

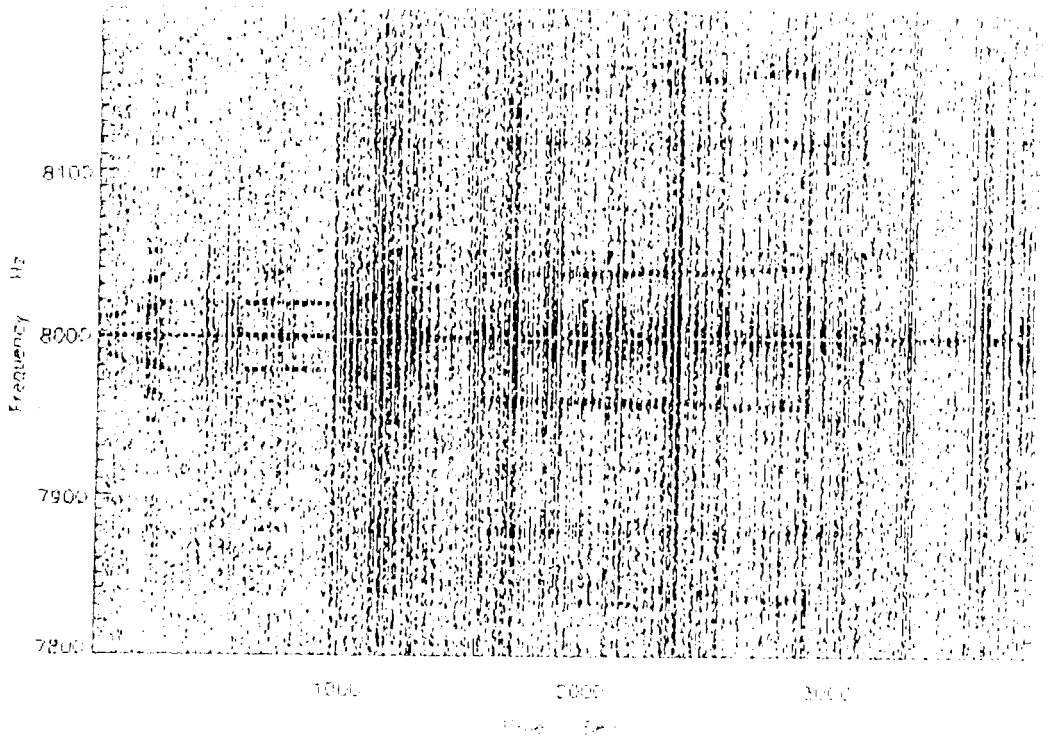

Figure 7. Time-frequency analysis of downlink data

EG&G APD was used at TMF for detecting the downlink signal. The APD current, after amplification, was sampled at the audio rate of 22 kHz primarily to observe the 8-kHz modulation.

With the effects of scintillation averaged out on the downlink, we expected a fairly stable downlink signal assuming that the pointing jitter would be small just as in the uplink. As Figure 6 shows, the peak received power was as high as 2.5 nW which agreed well with the numbers predicted by the link table but the downlink signal fluctuation was much larger than expected. Figure 6 shows a plot of the downlink signal versus time with each point representing the average of the signal over 1-second. The figure clearly shows deep low-frequency fades lasting several seconds to minutes. The 1-second-averaging of the signal in the plot hides both the 8-kHz modulation as well as higher frequency fades. Histograms of the downlink signal over several minutes show a characteristic drop-off at some power levels indicative of pointing jitter dominated distribution discussed in Section 3.1. When the downlink was stable, we observed bit-error-rates of less than 10^{-5} over several seconds. To further understand the causes of the signal variations we performed various frequency and time-frequency analysis.

Fast Fourier Transforms (FFTs) of the downlink signal showed several distinctive peaks in addition to the clear peak at 8-kHz depending on the data format ("E2", PN or regeneration) used [3]. The FFT analysis of the downlink signal further showed small components at tens of Hz. Time frequency analysis of the signal provided information on how these low frequency component changed with time. Figure 7 shows the evolution of low frequency components with time around the carrier frequency of 8-kHz. Each vertical line in the figure represents FFT of data from a 1-sec interval. One can easily discern distinct signal components starting at 10 Hz which slowly change in frequency to 20 Hz. The 20-Hz signal was stable for several minutes and then drifted towards 60 Hz. Occasionally we saw harmonics of these low frequency components. The origin of the 10-100 HZ signal and the reasons for the frequency change are not completely understood. The fact that the components are sharp and symmetric about the carrier frequency of 8-kHz suggest that the origin of the low-frequency fluctuations was the LCE or the satellite itself. The slow change in frequency could be due to change or drift in temperature resulting in drift in the modes of vibration. In any case, the severe signal variations limited collection of "E2" and "PN" data from the optical signal.

4. CONCLUSIONS

Predicted and measured values of the mean received power, both 011 uplink and downlink, agreed well (within ± 3 dB) given the uncertainty in the optical losses of telescopes at TMF and the actual atmospheric transmission. On the uplink, results from this paper and past analysis clearly confirm that multiple-beam uplink can significantly reduce signal fluctuations caused by scintillation. The observed variance of signal fluctuation on the uplink was lower than

expected while the variance of the signal on the downlink was significantly larger than expected. Downlink signal fluctuations are attributed to pointing jitter suggesting the need for highly accurate pointing to establish stable communication link.

ACKNOWLEDGEMENTS

The authors wish to thank the members of the GOLD team and the scientists at the Communications Research Laboratory involved in the experiments for their cooperation. The work described in this article was performed by the Jet Propulsion Laboratory, California Institute of Technology, under contract with the National Aeronautics and Space Administration.

REFERENCES

1 K. Wilson, ""An overview of the GOLD experiment between the ETS-VI satellite and the Table Mountain Facility"," *The Telecommunications and Data Acquisition Progress Report* **42-124**, February 15 1996.

2 K. Wilson, J. Lesh, K. Araki, and Y. Arimoto, ""Preliminary results of the GOLD experiment Table Mountain Facility and the ETS-VI satellite"," *SPIE Proceedings* **2699**, pp. 121–132, 1996.

3 K. Wilson, M. Jeganathan, J. R. Lesh, J. James, and G. Xu, ""Results from phase-1 and phase-2 GOLD experiments"," *The Telecommunications and Data Acquisition Progress Report* **42-128**, February 15 1997.

4 Y. Arimoto, M. Toyoshima, M. Toyoda, T. Takahashi, M. Shikatani, and K. Araki, ""Preliminary result on laser communication experiment using ETS-VI"," *SPIE Proceedings* **2381**, pp. 151–158, 1995.

5 J. W. Goodman, *Statistical Optics*, New York: John Wiley and Sons, 1985.

6 R. E. Hufnagel, ""Variations of Atmospheric Turbulence"," in *Digest of Topical Meeting on Optical Propagation Through Turbulence*, Optical Society of America, Washington, D.C., 1974. paper WA1.

7 G. C. Valley, ""Isoplanatic degradation of tilt correction and short-term imaging systems"," *Appl. Opt.* **19**, p. 574, 1980.

8 F. G. S. (editor), *Atmospheric Propagation of Radiation, Vol. 2*, SPIE Optical Engineering Press, Bellingham, 1993.

9 W. L. Wolfe and G. J. Z. (editors), *The Infrared Handbook*, Environmental Research Institute of Michigan, revised ed., 1989.

10 L. C. Andrews and R. L. Phillips, ""I-K distribution as a universal propagation model of laser beams in atmospheric turbulence"," *J. Opt. Soc. Am. A* **2**, p. 160, 1985.

11 L. C. Andrews, R. L. Phillips, and B. K. Shivamogg, ""Relations of the parameters of the I-K distribution for irradiance fluctuations to physical parameters of the turbulence"," *Appl. Opt.* **27**, p. 2150, 1985.

12 V. I. Tatarskii, *Wave Propagation in Turbulent Medium*, New York: McGraw-Hill, 1961.

13 A. Ishimaru, *Wave Propagation and Scattering in Random Media, Vol. 2*, New York: Academic Press, 1978.

14 S. Clifford, G. R. Ochs, and R. S. Lawrence, ""Saturation of optical scintillation by strong turbulence"," *J. Opt. Soc. Am.* **64**(148), 1974.

15 M. Jeganathan, K. E. Wilson, and J. R. Lesh, ""Preliminary analysis of fluctuations in the received uplink-beacon-power data obtained from the GOLD experiments"," *The Telecommunications and Data Acquisition Progress Report* **42-124**, pp. 20–32, February 15 1996.

16 M. Toyoshima, K. Araki, Y. Arimoto, M. Toyoda, M. Jeganathan, K. Wilson, and J. R. Lesh, ""Reduction of ETS-VI laser communication equipment optical-downlink telemetry collected during GOLD"," *The Telecommunications and Data Acquisition Progress Report* **42-128**, February 15 1997.

17 K. Kiasaleh and T.-Y. Yan, ""A statistical model for evaluating GOPEX uplink performance"," *The Telecommunications and Data Acquisition Progress Report* **42-111**, 1992.